AIP | Advances

Thermal expansion accompanying the glass-liquid transition and crystallization

M. Q. Jiang, M. Naderi, Y. J. Wang, M. Peterlechner, X. F. Liu, F. Zeng, F. Jiang, L. H. Dai, and G. Wilde

Citation: AIP Advances **5**, 127133 (2015); doi: 10.1063/1.4939216
View online: http://dx.doi.org/10.1063/1.4939216
View Table of Contents: http://scitation.aip.org/content/aip/journal/adva/5/12?ver=pdfcov
Published by the AIP Publishing

AIP ADVANCES **5**, 127133 (2015)

Thermal expansion accompanying the glass-liquid transition and crystallization

M. Q. Jiang,[1,2,a] M. Naderi,[2] Y. J. Wang,[1] M. Peterlechner,[2] X. F. Liu,[1] F. Zeng,[1] F. Jiang,[3] L. H. Dai,[1,a] and G. Wilde[2]
[1]*State Key Laboratory of Nonlinear Mechanics, Institute of Mechanics, Chinese Academy of Sciences, Beijing 100190, China*
[2]*Institute of Materials Physics, Westfälische Wilhelms-Universität Münster, Münster 48149, Germany*
[3]*State Key Laboratory for Mechanical Behavior of Materials, Xi'an Jiaotong University, Xi'an 710049, China*

(Received 20 November 2015; accepted 15 December 2015; published online 24 December 2015)

We report the linear thermal expansion behaviors of a Zr-based (Vitreloy 1) bulk metallic glass in its as-cast, annealed and crystallized states. Accompanying the glass-liquid transition, the as-cast Vitreloy 1 shows a continuous decrease in the thermal expansivity, whereas the annealed glass shows a sudden increase. The crystallized Vitreloy 1 exhibits an almost unchanged thermal expansivity prior to its melting. Furthermore, it is demonstrated that the nucleation of crystalline phases can induce a significant thermal shrinkage of the supercooled liquid, but with the growth of these nuclei, the thermal expansion again dominates. These results are explained in the framework of the potential energy landscape, advocating that the configurational and vibrational contributions to the thermal expansion of the glass depend on both, structure and temperature.
[http://dx.doi.org/10.1063/1.4939216]

The complexity of the glass transition is reflected by both, the slowing down of dynamics and the ergodicity breaking of thermodynamics.[1] Analyzing the changes of dynamic/thermodynamic properties accompanying the glass transition in turn opens a window into understanding the glass-liquid transition process and even the nature of glasses.[2,3] Recently, the thermal expansion of glasses has drawn increasing attention due to its relation to the free volume[4–6] or vacancy[7] kinetics, glass transition temperature,[8,9] kinetic fragility,[10,11] glass forming ability,[6,12] etc. It is well known that the thermal expansion of crystals is mainly determined by the anharmonicity of the atomic vibrations. As for glasses, however, the disordered configuration offers an additional contribution to their thermal expansion.[12,13] This additional configurational contribution usually produces the experimentally familiar jump in the thermal expansivity upon heating a glass into its supercooled liquid.[3,4,14–16] On the other hand, the opposite situation can be also observed: the thermal expansivity displays a continuous decrease as the glass-liquid transition occurs.[9,11,17,18] The precise picture of how the thermal expansion evolves with the glass-liquid transition and even the subsequent crystallization, therefore, remains unclear and deserves specific investigation.

In this paper, we performed measurements of the linear thermal expansion on a typical Zr-based (Vitreloy 1) bulk metallic glass over a wide range of temperatures. By pre-annealing, we captured two contrary scenes, as mentioned above, of the thermal expansion accompanying the glass-liquid transition of the same composition. Furthermore, the thermal shrinkage/expansion of the supercooled liquid during the subsequent crystallization was revealed. All of the obtained results are in line with the potential energy landscape (PEL) approach.

[a]Authors to whom correspondence should be addressed. Electronic addresses: mqjiang@imech.ac.cn; lhdai@lnm.imech.ac.cn

Vitreloy 1,[19] with a norminal composition of $Zr_{41.2}Ti_{13.8}Cu_{12.5}Ni_{10.0}Be_{22.5}$ (at.%), was chosen as a model glass. Linear thermal expansion measurements were performed by using a Dilatometer (Linseis) on the as-cast glassy (Zr^{ac}), annealed glassy (Zr^{an}) and fully crystallized (Zr^{cr}) states of Vitreloy 1. The annealed glassy states were obtained by heating the as-cast Vitreloy 1 up to 623 K in a pure argon atmosphere at a heating rate of 5 K/min, and subsequent cooling to room temperature at the same rate. Fully crystallized samples were prepared by heating the as-cast Vitreloy 1 up to 773 K in a pure argon atmosphere at a heating rate of 5 K/min, followed by isothermal annealing for 1 hour, and subsequent cooling to room temperature at the same rate. The three states of Vitreloy 1 (Zr^{ac}, Zr^{an} and Zr^{cr} denoting the as-cast, annealed and crystallized states, respectively) were well characterized by X-ray diffraction (XRD)[20] and differential scanning calorimetry (DSC), as shown in Fig. 1(a). The DSC traces indicate that at a heating rate of 20 K/min, both Zr^{ac} and Zr^{an} glasses underwent three characteristic thermodynamic events: the glass transition, crystallization and melting, whereas the crystallized Zr^{cr} alloy only showed the endothermic peaks of melting. According to the exothermic enthalpy before the glass transition (see the inset in Fig. 1(a)), the relative amount of excess free volume can be estimated as 100%, 50% and 0%, respectively, in the Zr^{ac}, Zr^{an} and Zr^{cr} states. The 50% reduction of relative free volume leads to an earlier crystallization; the onset temperatures of crystallization T_{cr}^{onset} are 698 K and 693 K for the Zr^{ac} and Zr^{an} glasses, respectively. However, as expected, the glass transition occurs in the same temperature range with the glass

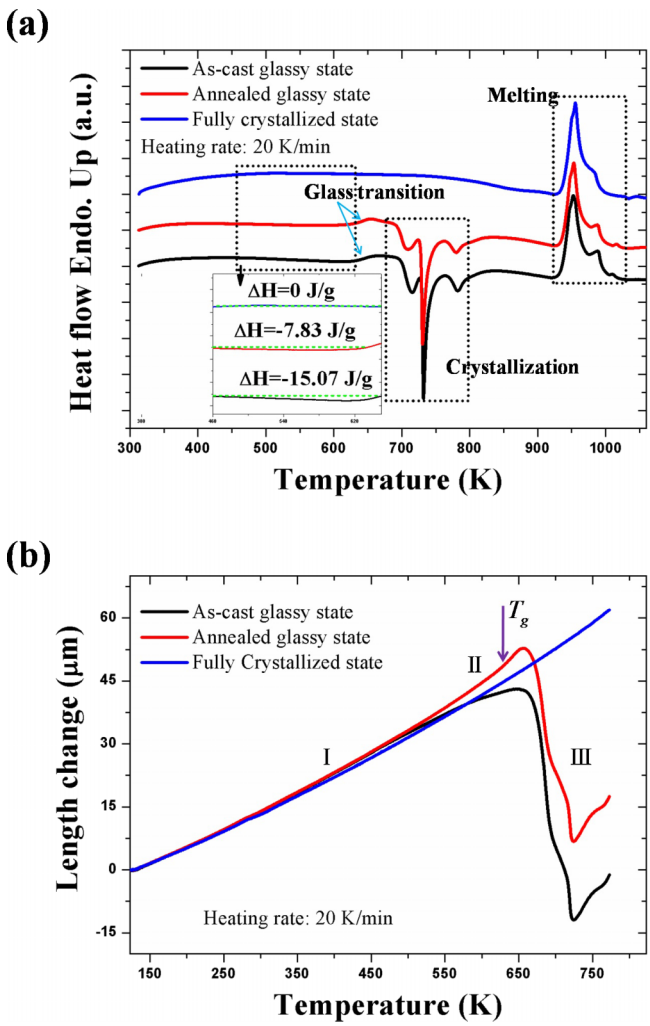

FIG. 1. (a) DSC traces and (b) linear thermal expansion curves of the as-cast glassy, annealed glassy, and crystallized Vitreloy 1.

transition temperature, T_g, about 623 K, and the onset and end temperatures are about 593 K and 638 K, respectively. The different relaxational states are indicated by the different height of the maximum at the glass transition. Rectangular samples with dimensions of $3 \times 3 \times 10$ mm^3 were used for the dilatometric measurements. The temperature range for measurements was chosen from 123 K to 773 K, and the heating rate was kept constant at 20 K/min.

Figure 1(b) presents the typical curves of the linear thermal expansion for Vitreloy 1 in the as-cast glassy, annealed glassy and crystallized states. For the two glassy states (Zr^{ac} and Zr^{an}), the relationship between sample length change and temperature can be roughly divided into three regimes. In regime I, the thermal expansion is nearly linear up to a temperature below the onset temperature of the glass transition. In regime II, the glass-liquid transition occurs, and the accompanying thermal expansion exhibits an obvious departure from its low-temperature linear behavior. Regime III corresponds to the viscous flow and crystallization of supercooled liquid, during which the sample length firstly undergoes a significant decrease to a local minimum, and then re-increases with increasing temperature. In sharp contrast with the glassy states, the crystallized Vitreloy 1 (Zr^{cr}) shows an approximately linear increase of length within the whole temperature range of the measurement. In regime I, the average linear thermal expansion coefficients α can be determined as $(8.88 \pm 0.64) \times 10^{-6}$ K^{-1}, $(8.83 \pm 0.67) \times 10^{-6}$ K^{-1} and $(8.54 \pm 0.72) \times 10^{-6}$ K^{-1}, respectively for the as-cast glassy, annealed glassy and fully crystallized Vitreloy 1. These values are comparable to other measurements.[14,21] It is noteworthy that significantly structural relaxation or crystallization (Fig. 1(a)) only results in a very slight decrease of α below T_g (Fig. 1(b)). This demonstrates that the thermal expansion of glassy solids is mainly dominated by the anharmonicity of thermal vibrations, and the configurational or free volume change plays only a minor role.

To better understand the exact relationship between the thermal expansion and the glass-liquid-crystal transitions, we carried out a careful comparison between the length changes and the DSC traces in the temperature range between 450-773 K (covering regimes II and III), as shown in Fig. 2. It can be seen from Fig. 2(a) that for the as-cast Vitreloy 1 glass, the curve of length change versus temperature exhibits a gradually dipping slope across T_g. This indicates that the thermal expansion coefficient reduces when the as-cast glass transforms into its supercooled liquid state upon heating. Similar phenomena have been observed in Sm-based,[18] Gd-based,[11] Pd-based[5,6,9] and Fe-based[6] metallic glasses. Very differently, for the annealed Vitreloy 1 glass (Fig. 2(b)), the thermal expansivity shows an obvious increase by a factor of about 2 times when undergoing the glass-liquid transition, corresponding to a nonlinearly enhanced expansion. This type of thermal expansion behavior has been widely reported for various glass systems.[3,5,14,15] Herein, by performing a proper pre-annealing of an as-cast Vitreloy 1 glass, we reproduced two different, yet typical thermal expansion behaviors across T_g. It is found that whether the thermal expansion coefficient increases or decreases upon heating a glass into its supercooled liquid depends closely on the initial free volume in the glass. If the amount of free volume is high, the enhancement of the thermal expansion when entering the state of the supercooled liquid will be weakened. If the amount of free volume is comparably low (e.g., by pre-annealing), the glass-liquid transition will increase the thermal expansion coefficient significantly.

With further increasing the temperature into regime III, the supercooled liquid, from either the as-cast or the annealed glass, displays a drastic length change, which is indicated by a remarkable shrinkage, followed by expansion at higher temperatures. We note that the length shrinkage can even occur before the onset of crystallization. It is believed that the reason for this observed shrinkage is related to viscous flow of the supercooled liquid due to a combined effect of the increased temperature (above T_g) and a very small applied pressure of 30 mN during the dilatometer measurements. The compressive deformations were about 36.5 μm and 26.3 μm for the Zr^{ac} and Zr^{an} liquids, respectively. The crystallization further decreased the sample length, and the onset temperature of crystallization just corresponds to the change of the slope of the shrinkage curve. It is interesting to observe that a decrease of the length only occurred during the first step of crystallization; the thermal expansion become again positive at the beginning of the second step of crystallization. As indicated by Fig. 1(a), both Zr^{ac} and Zr^{an} liquids experienced a three-step crystallization process, corresponding to three sequential exothermic peaks. The first step was identified as the nucleation of icosahedral phases, and the following two steps were related to the formation

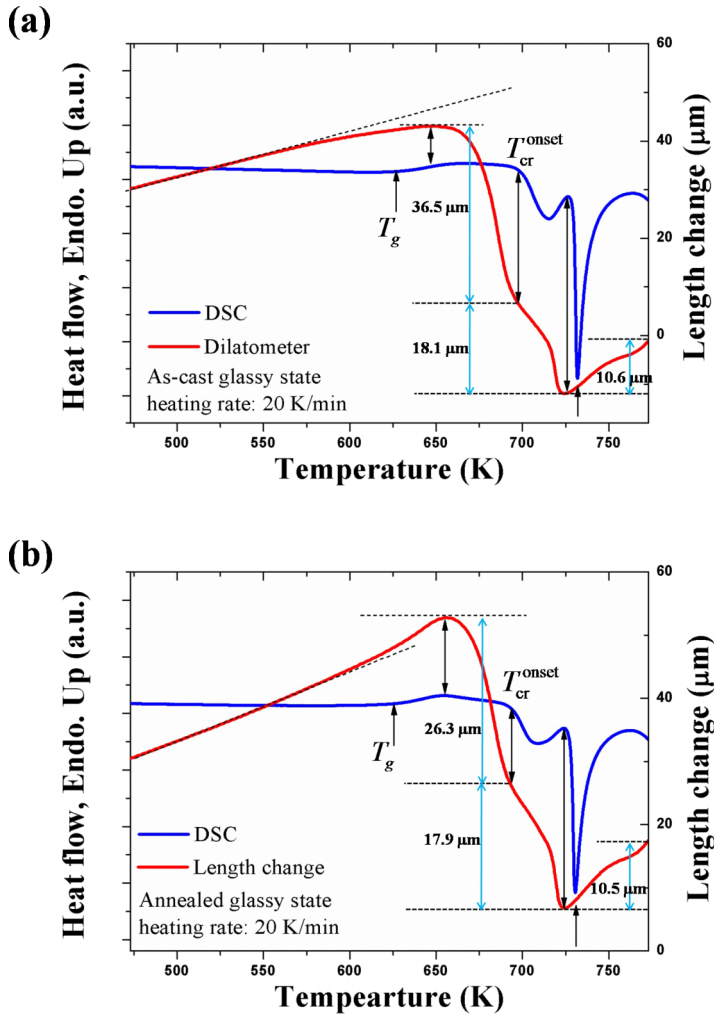

FIG. 2. Comparison between DSC trace and linear thermal expansion of (a) the as-cast glassy and (b) the annealed glassy Vitreloy 1 across the glass-liquid transition and subsequent crystallization.

of intermetallic compounds.[22,23] These compounds should be similar to the crystallization products marked in the XRD pattern of the Zr^{ac} alloy.[20]

For confirmation, the Zr^{ac} liquid was configurationally frozen-in at 725 K by the water quenching method and the microstructure was then observed by transmission electron microscopy.[20] It is observed that many nanocrystals with an average size of about 30 nm are homogeneously distributed in the residual amorphous matrix. These nanocrystals that formed at a very high number density are most probably the result of the primary nucleation of an icosahedral phase in the first step. At higher temperatures and long times, these metastable quasicrystalline phase will transform to the final intermetallic compounds with an average size of about 100 nm at the end of the third transformation step.[22] These results provide important insight into the crystallization of supercooled liquid. Significant structural ordering is mainly ascribed to the nucleation of crystalline phases, which then, due to the associated volume change, dominates the thermal expansion signal. However, with decreasing amount of the amorphous phase fraction, the signal due to thermal expansion will dominate again. These results also confirm that the formation of icosahedral clusters leads to a highest packing density or a lowest free volume,[24] whereas structural disordering mainly results from the breakdown of these icosahedral clusters.[25] More interestingly, the absolute values of the length decrease or increase are almost identical during the crystallization of the two supercooled liquids (Zr^{ac} and Zr^{an}), as marked in Fig. 2. This implies that the thermal shrinkage/expansion of the supercooled liquid due to crystallization does not depend on the initial structure of the glass, although

the onset of the crystallization itself is structure-dependent (Fig. 1(a)). This behavior indicates that crystallization under such conditions involves transient states and is distinctly time-dependent.

The observed thermal expansion behavior during the glass-liquid-crystal transition can be interpreted in the framework of PEL.[1,26,27] The PEL is a multidimensional hyper-surface that describes the potential energy of an N-atomic glassy system $\Phi(\vec{r}_1,...,\vec{r}_N)$ as a function of the $3N$ configurational coordinates $\vec{r}_i$. The state of the system can be well represented by a point on or above the hyper-surface. By analogy to Earth's topography, Stillinger and Weber[27,28] carried out a formally exact partitioning of the configuration space as a sum of distinct basins, associating with each local minimum of the potential energy surface (named an inherent structure, IS). The landscape picture provides a natural separation of the atomic motion of the system into sampling distinct ISs and vibrations within an IS. Therefore, the vibrational and configurational contributions to the thermal expansion coefficient (α) can be unambiguously resolved.[13] The first ($\alpha_{\rm vib}$) originates from intra-IS anharmonic thermal vibrations; the second ($\alpha_{\rm con}$) arises from thermally induced structural explorations of the IS occupancies.

This idea is schematically illustrated in Fig. 3. At a temperature T well below T_g, the as-cast Zr^{ac} glass with a large amount of free volume resides in a high-energy level IS, and the atomic vibration in the IS is controlled by T. Compared to the as-cast Zr^{ac} glass, the annealed Zr^{an} glass is localized in a deeper IS due to the progressive exploration of deeper and deeper ISs during the long-time annealing. The crystallized Zr^{cr} alloy is confined in the deepest potential basin $e_{\rm cr}$. Since $T < T_g$, the configurational contribution $\alpha_{\rm con}$ is structurally frozen, but the vibrational component $\alpha_{\rm vib}$ that just depends on temperature still exists for the Zr^{ac} and Zr^{an} glasses and the crystallized Zr^{cr} alloy. It is obvious that within the deeper ISs, the anharmonicity of the thermal vibrations becomes weaker. This explains the observation that the thermal expansivity α decreases slightly in the order: Zr^{ac}, Zr^{an} and Zr^{cr} (region I in Fig. 1(b)).

As a glass passes upward in temperature through the glass transition, the configurational contribution $\alpha_{\rm con}$ to the thermal expansion will start to become significant. For the as-cast Zr^{ac} glass, the initial large amount of free volume allows for sampling a larger part of the PEL, which enhances the probability for the system to experience significant structural shifts involving deeper ISs. This process is activated by thermal fluctuation and thus is enhanced at increasing temperatures. This

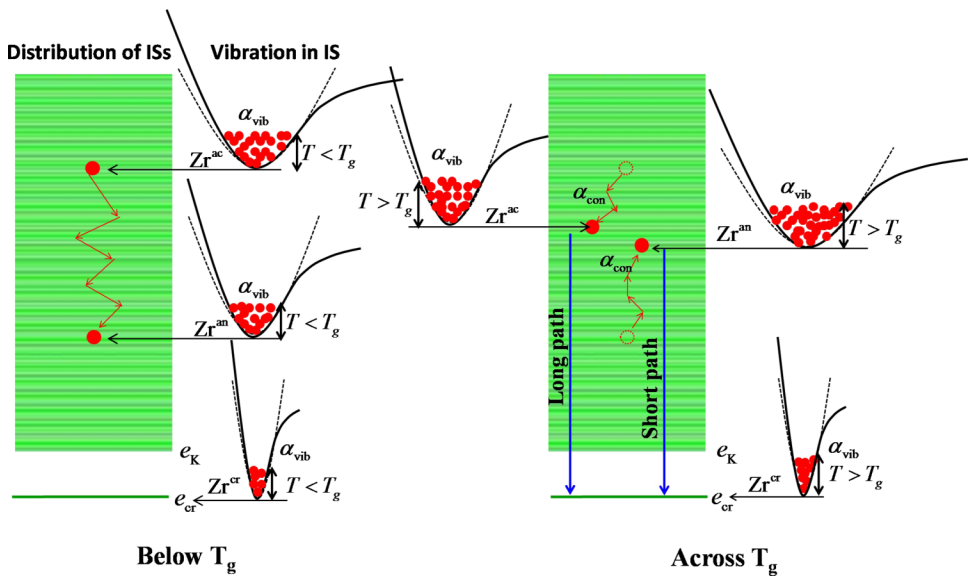

FIG. 3. The potential energy landscape for the as-cast glassy, annealed glassy, and crystallized Vitreloy 1 schematizing the vibrational and configurational contributions to thermal expansion below (left panel) and across (right panel) the glass-liquid transition. The distribution of inherent structures (ISs) indicates the possible values of energy of ISs, bounded from below by the lowest IS energy $e_{\rm K}$ of an ideal Kauzmann glass. The energy of the crystallized state IS is denoted by $e_{\rm cr}$. The vibration property in each IS is controlled by temperature.

behavior thus can result in a negative α_{con} that will counteract the positive vibrational contribution α_{vib} due to the increasing temperature. The total thermal expansivity α therefore shows a gradual decrease for the as-cast glass in the temperature range of glass transition, as experimentally observed in Fig. 2(a). In contrast, the annealed Zr^{an} glass that resides in a deeper IS within the PEL, upon identical thermal activation, is bound to sample ISs at higher energy levels, corresponding to an effective free volume increase. This leads to a positive configurational contribution α_{con} that will be superimposed on the enhanced vibrational contribution α_{vib}. Thus, a pronounced increase of the total thermal expansivity α can be observed through the glass-liquid transition, as shown in Fig. 2(b). In fact, the structural modifications observed here for the thermally induced glass-liquid transition are similar to these occurred during stress-driven yielding of glasses,[29,30] provided that the mechanical yielding is described as a stress-induced glass transition.[31,32] Very recently, Fan *et al.*[33] by molecular dynamics simulations have indeed revealed that atomic disordering (activation) and ordering (relaxation) events exist simultaneously in thermally activated deformation of metallic glasses.

Furthermore, based on the observation that the Zr^{an} liquid starts to crystallization at a lower onset temperature than the Zr^{ac} liquid (Fig. 1(a)), we can deduce that the free volume concentration in the former is lower than in the latter. This observation also indicates that the glass transition does not change the respective crystallization paths of both liquids (right panel in Fig. 3). The Zr^{an} liquid still maintains a shorter crystallization path, although the amount of free volume adjusts during the glass transition and thus prior to the onset of crystallization. This observation indicates the presence of structural units even in the as-cast glass that will develop with time to nucleation centers of even to nuclei, in general agreement with the basic assumptions of transient nucleation theories. This result also indicates, that the well-known bulk glass former Vitralloy 1 vitrifies by growth control unlike the Pd-based or Al-based bulk glass formers where purification treatments can yield nucleate-depleted melts that vitrify by avoiding nucleation.[34–36] For the crystallized Zr^{cr} alloy that resides within the deepest basin, the thermal vibrations of atoms are confined near the equilibrium position of the basin. Therefore, the anharmonicity of the atomic vibrations or the resultant thermal expansion cannot change significantly, as long as the temperature is well below the melting point of the system.

In summary, the linear thermal expansion of a Vitreloy 1 bulk metallic glass was determined experimentally in its as-cast, annealed and crystallized states over a wide range of temperatures from 123 K to 773 K. It was observed that thermally activated configurational changes lead to two contrary thermal expansion behaviors during the glass-liquid transition: a gradual decrease in α for the as-cast state and an obvious increase for the annealed state. The subsequent crystallization (nucleation and growth) of the supercooled liquid resulted in a thermal shrinkage followed by expansion at higher temperatures. The crystallized Vitreloy 1 shows an approximately linear increase of the sample length with increasing temperature up to 773 K. These results can be consistently interpreted in the framework of PEL approach, by distinguishing vibrational and configurational contributions to the thermal expansion.

M.Q.J. acknowledges the Alexander von Humboldt Foundation for support with a research fellowship. This work was supported by DFG, the National Nature Science Foundation of China (Grant Nos. 11522221, 11372315, 11472287 and 11402269), the National Basic Research Program of China (Grant No. 2012CB937500), and the CAS/SAFEA International Partnership Program for Creative Research Teams.

[1] P. G. Debenedetti and F. H. Stillinger, Nature **410**, 259 (2001).
[2] S. Sastry, P. G. Debenedetti, and F. H. Stillinger, Nature **393**, 554 (1998).
[3] J. C. Dyre, Rev. Mod. Phys. **78**, 953 (2006).
[4] I. R. Lu, G. P. Gorler, H. J. Fecht, and R. Willnecker, J. Non-Cryst. Solids **274**, 294 (2000).
[5] A. R. Yavari, A. Le Moulec, A. Inoue, N. Nishiyama, N. Lupu, E. Matsubara, W. J. Botta, G. Vaughan, M. Di Michiel, and A. Kvick, Acta Mater. **53**, 1611 (2005).
[6] Q. Hu, X.-R. Zeng, and M. W. Fu, J. Appl. Phys. **109**, 053520 (2011).
[7] F. Ye, W. Sprengel, R. K. Wunderlich, H. J. Fecht, and H. E. Schaefer, Proc. Natl. Acad. Sci. U. S. A. **104**, 12962 (2007).
[8] L. F. Chua, C. W. Yuen, and H. W. Kui, Appl. Phys. Lett. **67**, 614 (1995).
[9] H. Kato, H. S. Chen, and A. Inoue, Scr. Mater. **58**, 1106 (2008).
[10] P. Bordat, F. Affouard, M. Descamps, and K. L. Ngai, Phys. Rev. Lett. **93**, 105502 (2004).

[11] J. Guo, X. F. Bian, Y. Zhao, S. J. Zhang, T. B. Li, and C. D. Wang, J Phys-Condens Mat **19**, 116103 (2007).
[12] J. C. Bendert, A. K. Gangopadhyay, N. A. Mauro, and K. F. Kelton, Phys. Rev. Lett. **109**, 185901 (2012).
[13] F. H. Stillinger and P. G. Debenedetti, J. Phys. Chem. B **103**, 4052 (1999).
[14] Y. He, R. B. Schwarz, D. Mandrus, and L. Jacobson, J. Non-Cryst. Solids **205–207**, 602 (1996).
[15] N. Mattern, H. Hermann, S. Roth, J. Sakowski, M. P. Macht, P. Jovari, and J. Z. Jiang, Appl. Phys. Lett. **82**, 2589 (2003).
[16] N. Mattern, U. Kühn, H. Hermann, S. Roth, H. Vinzelberg, and J. Eckert, Mater. Sci. Eng. A **375–377**, 351 (2004).
[17] Y. Zhang, D. Q. Zhao, R. J. Wang, and W. H. Wang, Acta Mater. **51**, 1971 (2003).
[18] J. Guo, X. F. Bian, T. Lin, Y. Zhao, T. B. Li, B. Zhang, and B. A. Sun, Intermetallics **15**, 929 (2007).
[19] A. Peker and W. L. Johnson, Appl. Phys. Lett. **63**, 2342 (1993).
[20] See supplementary material at http://dx.doi.org/10.1063/1.4939216 for the XRD patterns for the as-cast glassy, annealed glassy and fully crystallized Vitreloy 1 and the TEM observation of the as-cast Vitreloy 1 liquid quenched from 725 K.
[21] K. Ohsaka, S. K. Chung, W. K. Rhim, A. Peker, D. Scruggs, and W. L. Johnson, Appl. Phys. Lett. **70**, 726 (1997).
[22] S. J. Chung, K. T. Hong, M. R. Ok, J. K. Yoon, G. H. Kim, Y. S. Ji, B. S. Seong, and K. S. Lee, Scr. Mater. **53**, 223 (2005).
[23] S. B. Qiu and K. F. Yao, J. Alloys Compd. **475**, L5 (2009).
[24] X. J. Liu, C. L. Chen, X. Hui, T. Liu, and Z. P. Lu, Appl. Phys. Lett. **93**, 011911 (2008).
[25] A. J. Cao, Y. Q. Cheng, and E. Ma, Acta Mater. **57**, 5146–5155 (2009).
[26] M. Goldstein, J. Chem. Phys. **51**, 3728 (1969).
[27] F. H. Stillinger and T. A. Weber, Science **225**, 983 (1984).
[28] F. H. Stillinger, Science **267**, 1935 (1995).
[29] Z. T. Wang, J. Pan, Y. Li, and C. A. Schuh, Phys. Rev. Lett. **111**, 135504 (2013).
[30] M. Q. Jiang, G. Wilde, and L. H. Dai, Mech. Mater. **81**, 72 (2015).
[31] P. F. Guan, M. W. Chen, and T. Egami, Phys. Rev. Lett. **104**, 205701 (2010).
[32] H. L. Peng, M. Z. Li, and W. H. Wang, Appl. Phys. Lett. **102**, 131908 (2013).
[33] Y. Fan, T. Iwashita, and T. Egami, Phys. Rev. Lett. **115**, 045501 (2015).
[34] H. W. Kui and D. Turnbull, Appl. Phys. Lett. **47**, 796 (1985).
[35] G. Wilde, G. P. Görler, R. Willnecker, and G. Dietz, Appl. Phys. Lett. **65**, 397 (1994).
[36] S. K. Das, J. H. Perepezko, R. I. Wu, and G. Wilde, Mater. Sci. Eng. A **304–306**, 159 (2001).